AN EXPERIMENTAL STUDY OF PROPAGATING SPHERICAL FLAMES IN UNCONFINED HYDROGEN-OXYGEN EXPLOSIONS

Shiotani, A.[1], Kim, W.[2] Mogi, T.[1] and Dobashi, R.[1]
[1] Department of Chemical System Engineering, The University of Tokyo, 7-3-1 Hongo, Bunkyo-ku, Tokyo, 113-8656, Japan, a-shiotani@g.ecc.u-tokyo.ac.jp
[2] Department of Mechanical Systems Engineering, Hiroshima University, 1-4-1 Kagamiyama, Higashi-Hiroshima, 739-8527, Japan, kimwk@hiroshima-u.ac.jp

ABSTRACT

The study to understand the flame propagation behaviors of hydrogen-oxygen explosions is required to make a precise risk assessment. Moreover, although research has investigated the propagating spherical flames in unconfined hydrogen-air explosions no study to date has examined the hydrogen-oxygen explosions. The spherical flame propagation in unconfined hydrogen-oxygen explosions have been investigated using a soap bubble method. In the present experiments, hydrogen-oxygen mixtures were filled in a 10 cm diameter soap bubble and ignited by an electric spark at the center. The flame propagation behaviors were measured by a high-speed Schlieren photography. The laminar burning velocities and critical flame radii for the onset of flame acceleration in unconfined hydrogen-oxygen explosions were estimated. Results demonstrated that the laminar burning velocities of hydrogen-oxygen mixtures were much faster than those of hydrogen-air mixtures. In addition, the shift value of maximum laminar burning velocity for hydrogen-oxygen mixtures towards a leaner equivalence ratio is observed. The experimental flame speeds for all experiments were increased owing to diffusional-thermal and Darrieus-Landau instabilities, although the measured flame radii were small. The critical flame radius corresponding to the onset of flame acceleration decreased with the decrease in equivalence ratio.

1 INTRODUCTION

In gas explosion, flame surface is disturbed and wrinkled due to flame instabilities, such as diffusional-thermal and Darrieus-Landau (DL) instabilities.[1] Diffusional-thermal instability is caused by the difference of the diffusion velocity between combustible gas and flammable gas. The effect of diffusional-thermal instability depends on Lewis number (*Le*), which is defined as the ratio of the Schmidt to the Prandtl number. When *Le* is smaller than 1.0, diffusional-thermal instability forces strongly.[2] DL instability occurs as a result of thermal volumetric expansion of burned gas, corresponding to the expansion ratio of the burned and the unburned mixture. As the expansion ratio of the gas mixture increases, the effect of DL instability becomes strong. When the flame front is wrinkled, the flame surface area increases and the flame propagation is accelerated.[3] To make a precise risk assessment, it is necessary to research the flame propagation behavior including flame acceleration.

Although there are many pieces of research on hydrogen-air gas explosion, no prior studies on hydrogen-oxygen explosion have examined. This has been previously assessed only to a very limited extent because the hydrogen-oxygen explosion causes very strong explosion compared to the hydrogen-air gas explosion. Moreover, although research has illuminated the intensity of blast wave from hydrogen-oxygen explosion no study to date has examined the flame propagation behaviors of the mixtures. In the present study, unconfined hydrogen-oxygen gas explosions at various equivalence ratios were investigated experimentally. The objective of this study is to investigate the flame propagation in hydrogen-oxygen gas explosion. In particular, the laminar burning velocity and the onset of flame acceleration in the hydrogen-oxygen mixtures were evaluated.

2 EXPERIMENTAL METHOD

In order to measure flame propagation in unconfined explosions, we used the soap bubble method [4]. Figure 1 shows the schematic of experimental apparatus. The experimental apparatus is composed of

the gas supplying system, the ignition system and the high-speed Schlieren photography system. H_2 and O_2 mixture was made in the mixing chamber and the composition of the gas mixture was calculated by measuring the partial pressure of each gas. A 10 cm diameter soap bubble with the gas mixture was constructed from the gas flow nozzle. Ignition was produced at the center of the bubble by an electric spark. The flame propagation was imaged with Schlieren photography and recorded by a high-speed camera (Phantom VEO410, NOBBYTECH) at 22000 frames per second.

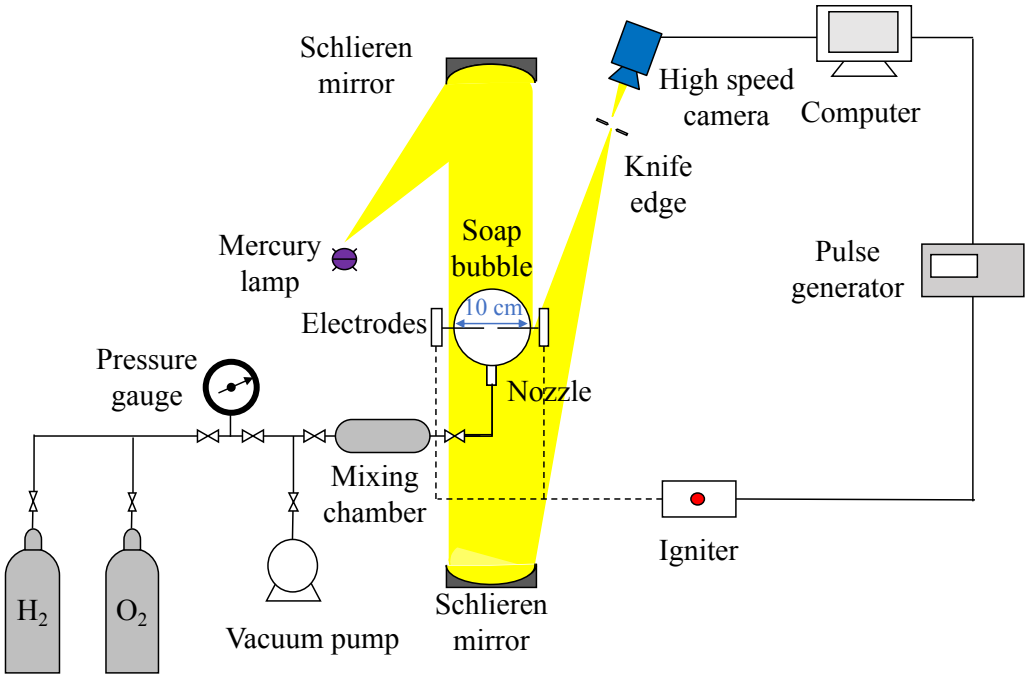

Fig. 1 Schematic of experimental apparatus

3 RESULTS AND DISCUSSIONS

The details of Schlieren images are shown in Fig. 2. The electrodes are inserted into the soap bubble and the hydrogen-oxygen mixtures at the center of the bubble were ignited by two 0.5 mm diameter electrodes in Fig. 2(a). The flame propagation behaviors were captured and the boundary between the flame and the bubble was visualized by Schlieren photography system in Fig. 2(b).

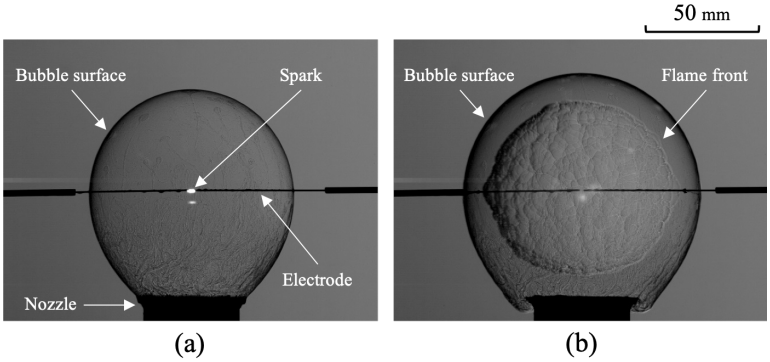

Fig. 2 Details of Schlieren image: (a) ignition, (b) flame propagation

Figure 3 shows the Schlieren images of outwardly propagating spherical flames for the hydrogen-oxygen mixture. The rapid development of cellular flame in the lean hydrogen-oxygen mixture was captured. As the equivalence ratio decrease, a cellularly unstable flame in the early stage of the

propagation is observed due to diffusional-thermal instability. In the present study, the flame area, A, is measured from the Schlieren images and the flame radius, r, is calculated from eq. (1).

$$r = \sqrt{\frac{A}{\pi}} \tag{1}$$

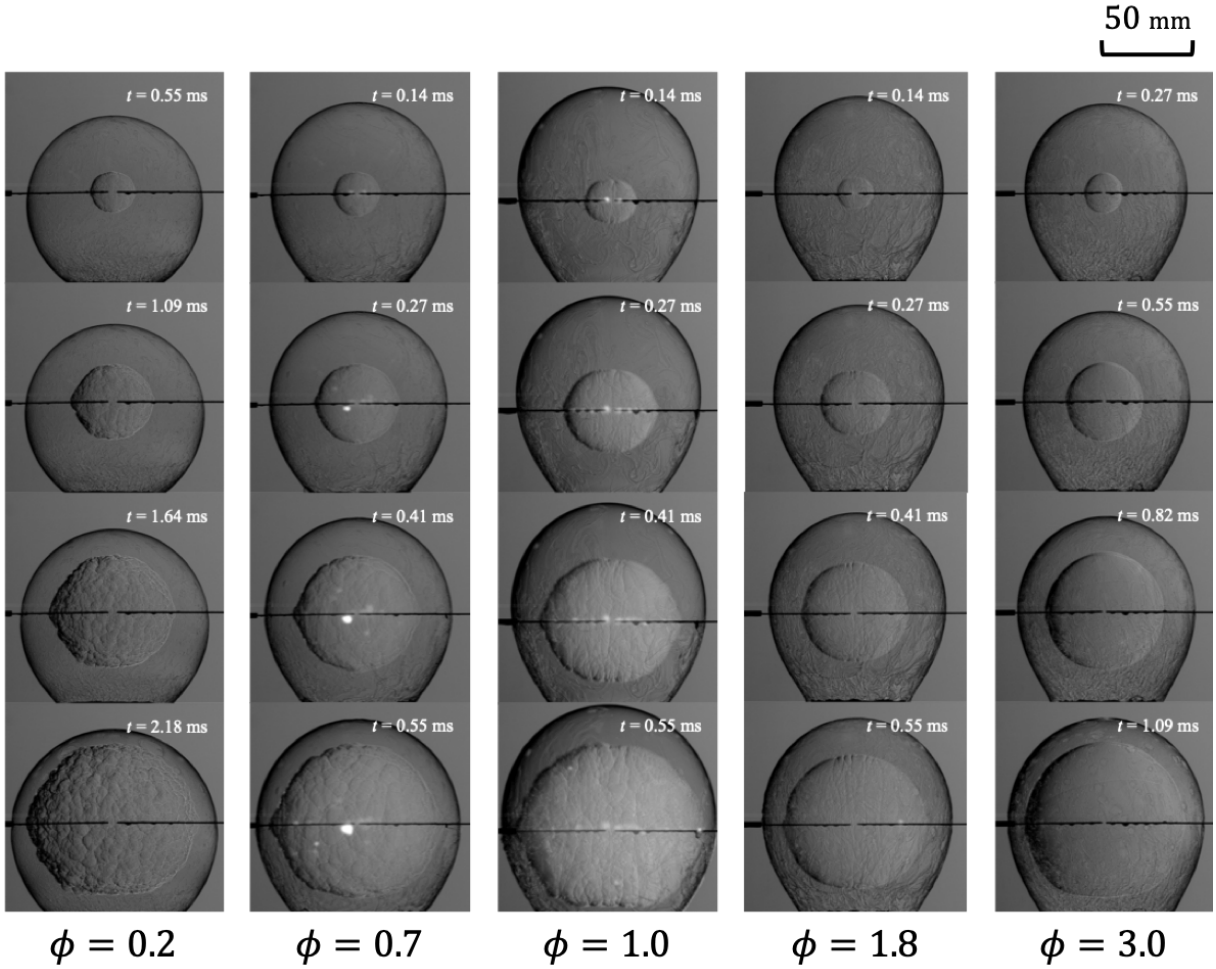

Fig. 3 Schlieren images at various equivalence ratios. : ϕ = equivalence ratio

The time histories of the flame radius and flame speed, V_f, at various equivalence ratios are shown in Figs. 4 and 5, respectively. Also, figure 6 shows that the relationship of the dimensionless flame speed to the dimensionless flame radius. The dimensionless flame speed is defined by the ratio of the flame speed to the unstretched laminar flame speed, $V_{L,}$. The dimensionless flame radius is defined by the ratio of the flame radius to the laminar flame thickness, δ, corresponding to the Péclet number, $Pe = r/\delta$. The unstretched laminar flame speed and the laminar flame thickness were calculated by CHEMKIN.

When the equivalence ratios are 0.2, 0.7, 1.0 and 1.8, the dimensionless flame speed increases and reaches more than 1.0 as the dimensionless flame radius becomes larger. Although, when the equivalence ratio is 3.0, the dimensionless flame speed is stable and does not reach 1.0. This is because the rich hydrogen flame was cellularly stable for $Le > 1$ mixtures. The value of dimensionless flame speed in ultra-lean mixtures with $\phi = 0.2$ is greater than 1.0 in the early stage of the propagation, because the effect of the diffusional-thermal instability leading to diffusively unstable flame for $Le < 1$ mixtures.

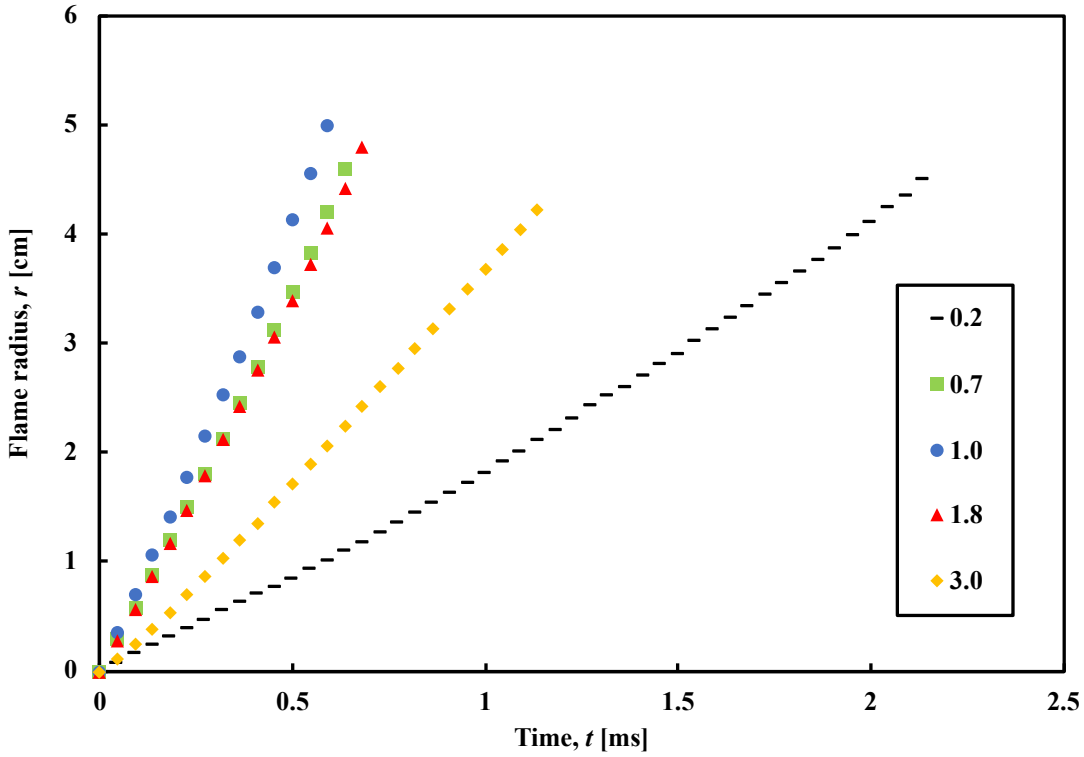

Fig. 4 Time histories of flame radius at various equivalence ratios.

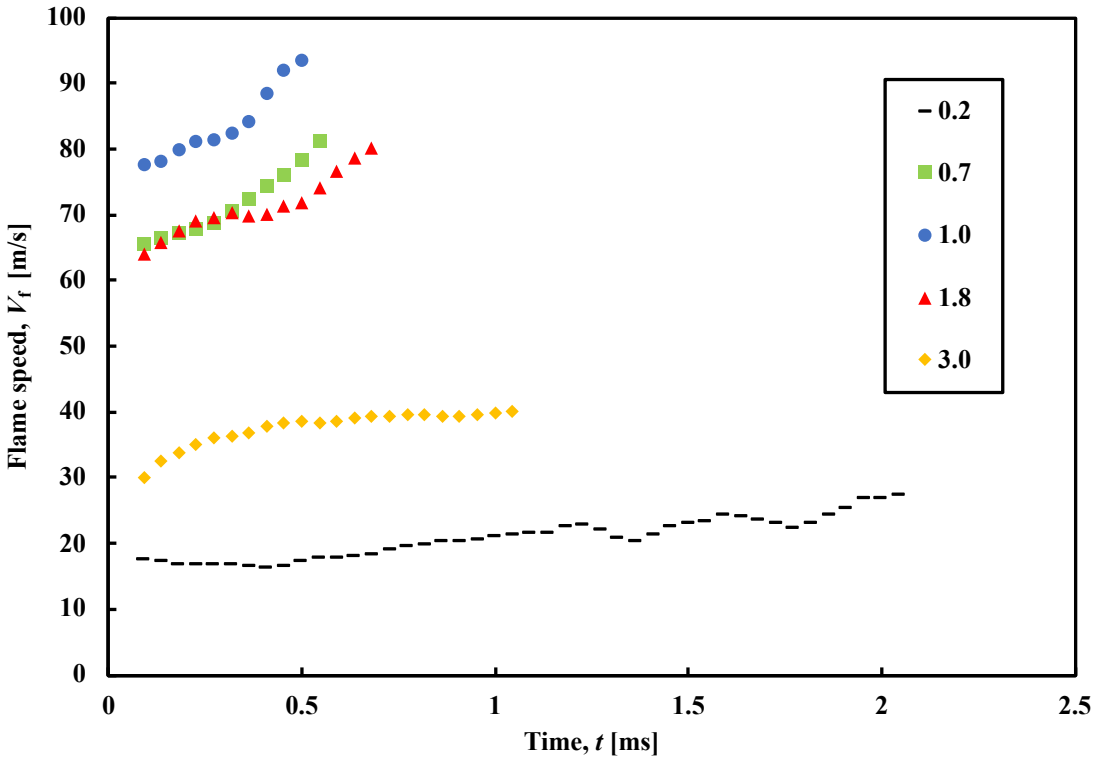

Fig. 5 Time histories of flame speed at various equivalence ratios.

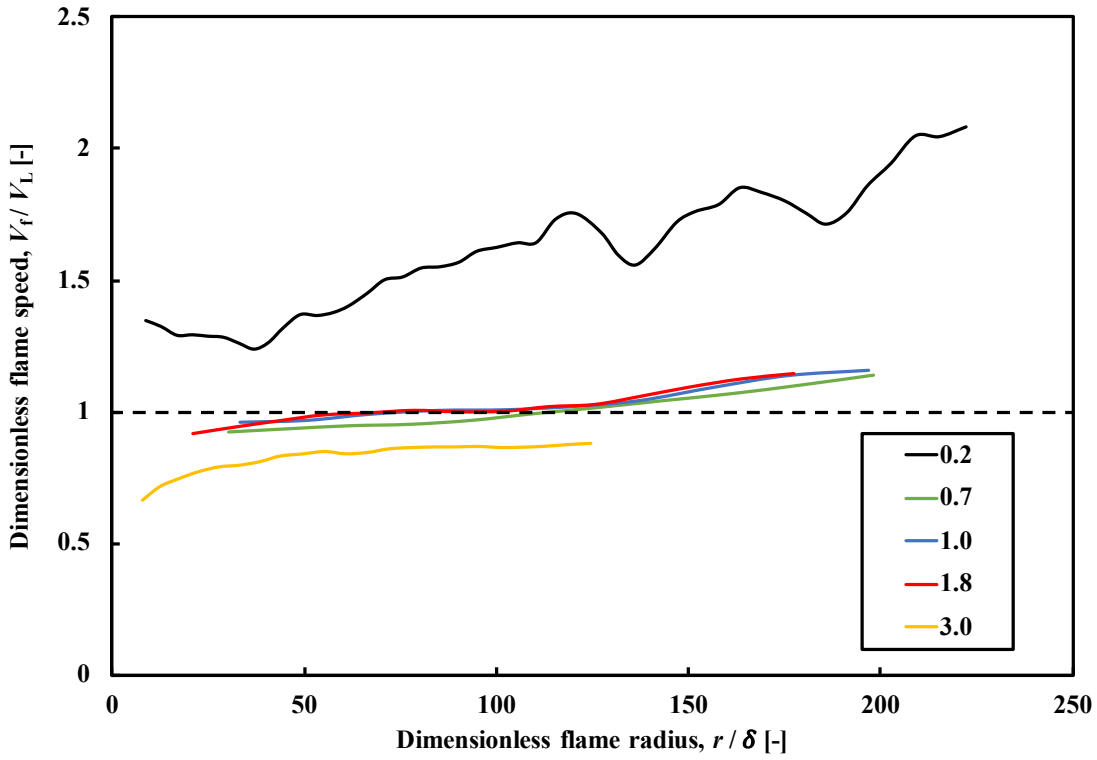

Fig. 6 Dimensionless flame speed versus dimensionless flame radius.

The relationship of the flame stretch rate to the flame speed is shown in Fig. 7. The flame stretch rate, K is calculated by eq. (2).

$$K = 2\frac{V_f}{r} \tag{2}$$

A linear relationship holds between the flame stretch rate and the flame speed as the following equation.[5-6]

$$V_L - V_f = L_b K \tag{3}$$

where V_L is the unstretched laminar flame speed, and L_b is the Markstein length. The orange line in Fig. 7 shows the linear relationship between the flame stretch rate and the flame speed before flame acceleration. According to eq. (3), the y-intercept of the orange line means the unstretched laminar flame speed and the gradient means the Markstein length. Also, the beginning of flame acceleration is the point where the linear relationship of eq. (3) does not hold. The flame radius at the onset of flame acceleration is defined as the critical flame radius, r_c and it can be obtained from Fig. 7.[7-11] The laminar burning velocity can be calculated as

$$S_L = \frac{\rho_b}{\rho_u} V_L \tag{4}$$

Herein, S_L is the laminar burning velocity, ρ_b is the density of burned gas, and ρ_u is the density of unburned gas.

Figure 8 shows the relationship of the Markstein length to the equivalence ratio. As the equivalence ratio decreases, the Markstein length also decreases. This decreasing tendency of Markstein length with the equivalence ratio was similar to that of hydrogen-air mixtures.

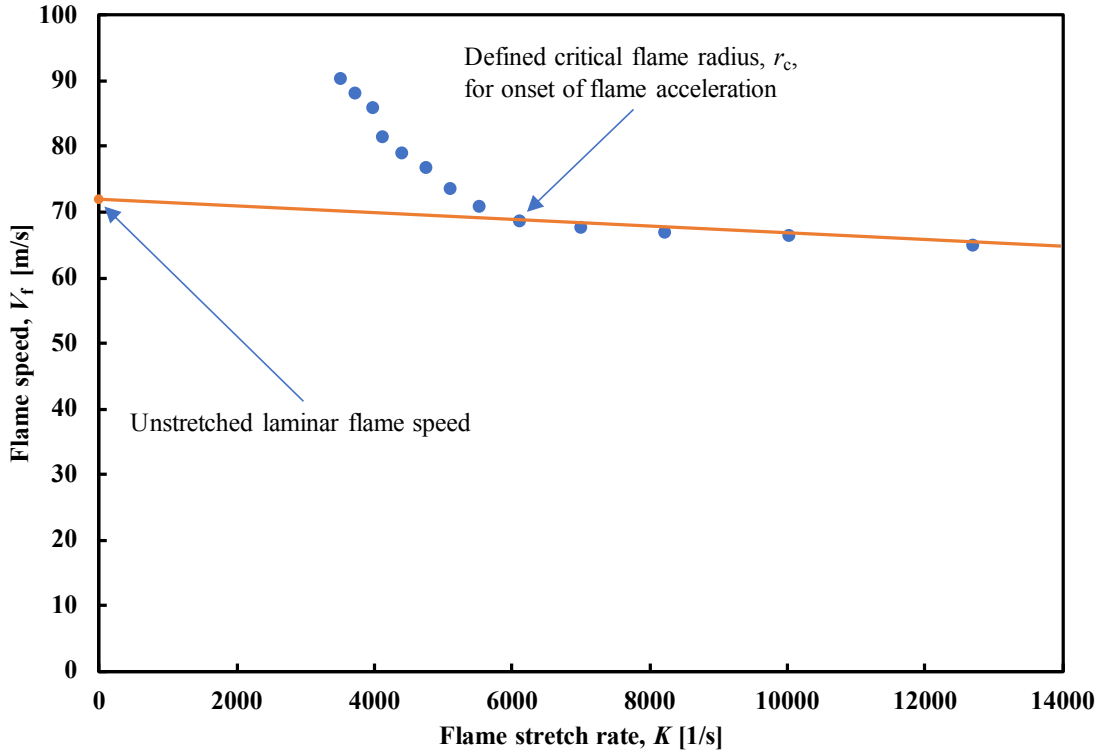

Fig. 7 Flame speed as a funtion of flame stretch rate. : $\phi = 0.7$

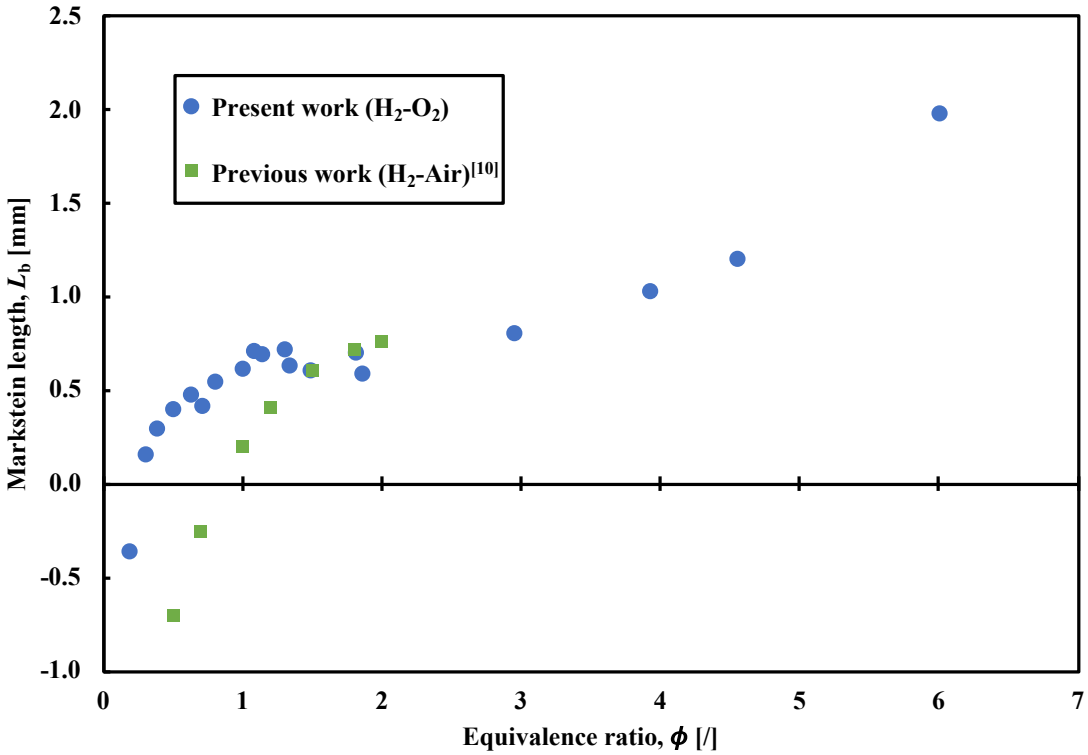

Fig. 8 Markstein length versus equivalence ratio.

The critical flame radius for the onset of flame acceleration as a function of the equivalence ratio is shown in Fig. 9. As the equivalence ratio decreases, the critical flame radius also decreases. Also, the critical flame radius in hydrogen-oxygen mixtures is smaller than in hydrogen-air mixtures. This is because the effect of diffusional-thermal instability forces strongly and the flame is accelerated at early time in the lean hydrogen-oxygen mixture. Also, in the present experiments, when the equivalence ratio is larger than 2.0, the critical flame radius is not obtained because the flame acceleration is not observed.

Figure 10 shows the laminar burning velocity as a function of the equivalence ratio. The experimental values of the velocity are compared with those calculated by using Chemkin-Pro with GRI Mech 3.0 reaction model. A good agreement between the experimental and calculated values was observed. The values of laminar burning velocity in hydrogen-oxygen mixtures reaches a maximum (about10 m/s) at the near-stoichiometric mixture, although the maximum value of hydrogen-air mixtures peak on the rich side. The maximum velocity in hydrogen-oxygen mixtures is about 3 times faster than that of hydrogen-air mixtures.

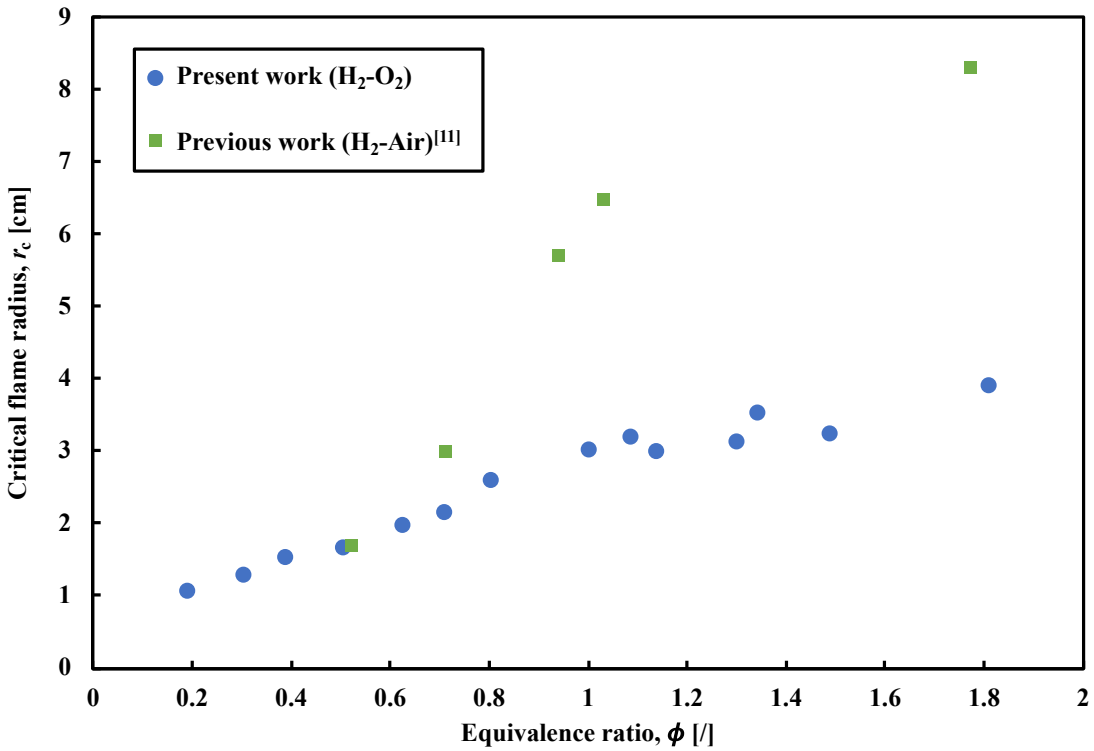

Fig. 9 Critical flame radius as a function of equivalence ratio.

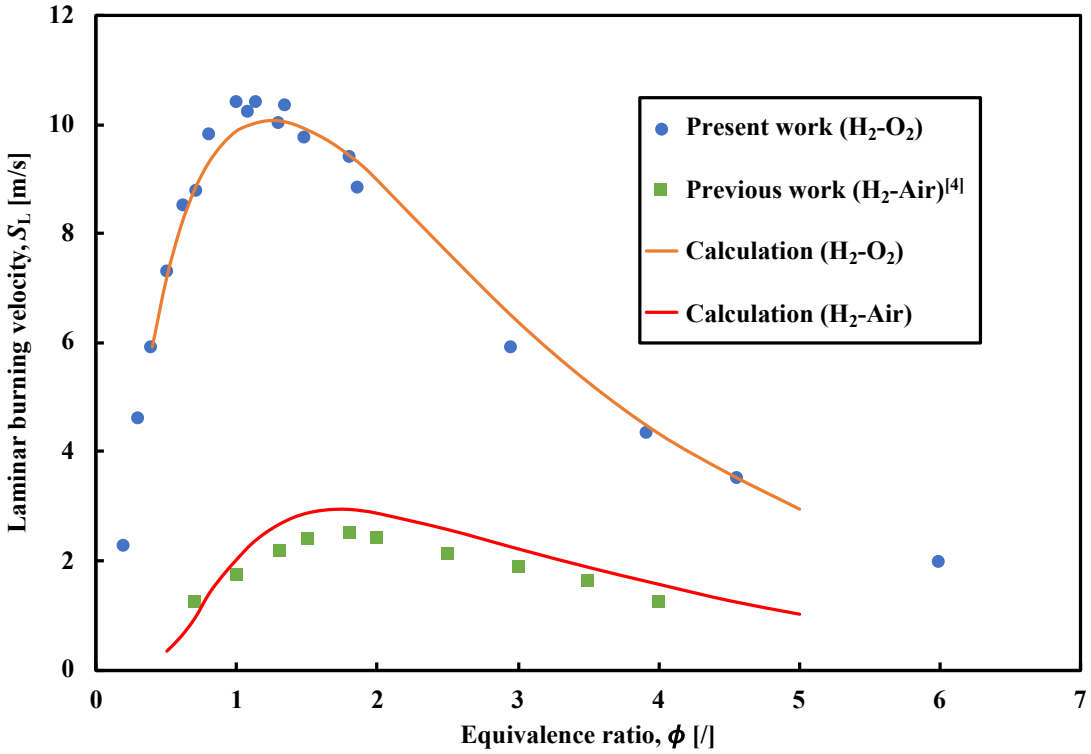

Fig. 10 Laminar burning velocity versus equivalence ratio.

The Zeldovich number, Ze, has been defined by

$$Ze = 4\frac{(T_a - T_u)}{(T_a - T_0)} \tag{5}$$

where T_a is the adiabatic flame temperature, and T_0 is the inner layer flame temperature.[12] The effective Lewis number, Le_{eff}, that is indicated as the intensified effect of the diffusional-thermal instability for $Le_{eff} < 1$ is calculated as

$$\begin{aligned} Le_{eff} &= 1 + \frac{(Le_E - 1) + (Le_D - 1)\{1 + Ze(1/\phi - 1)\}}{2 + Ze(1/\phi - 1)} && (\phi \le 1) \\ Le_{eff} &= 1 + \frac{(Le_E - 1) + (Le_D - 1)\{1 + Ze(\phi - 1)\}}{2 + Ze(\phi - 1)} && (\phi > 1) \end{aligned} \tag{6}$$

where Le_E is the Lewis number of excess reactant, and Le_E is the deficient reactant.[13]

Figure 11 shows the effective Lewis number as a function of equivalence ratio. In the lean hydrogen-oxygen mixtures, the effective Lewis number is smaller than 1.0, and the effect of diffusional-thermal instability is intensified. On the other hand, in the rich hydrogen-oxygen mixtures, the effective Lewis number is about 1.0, and the effect of diffusional-thermal instability does not force. Therefore, as the equivalence ratio decreases, a cellularly unstable flame in the early stage of the propagation is observed.

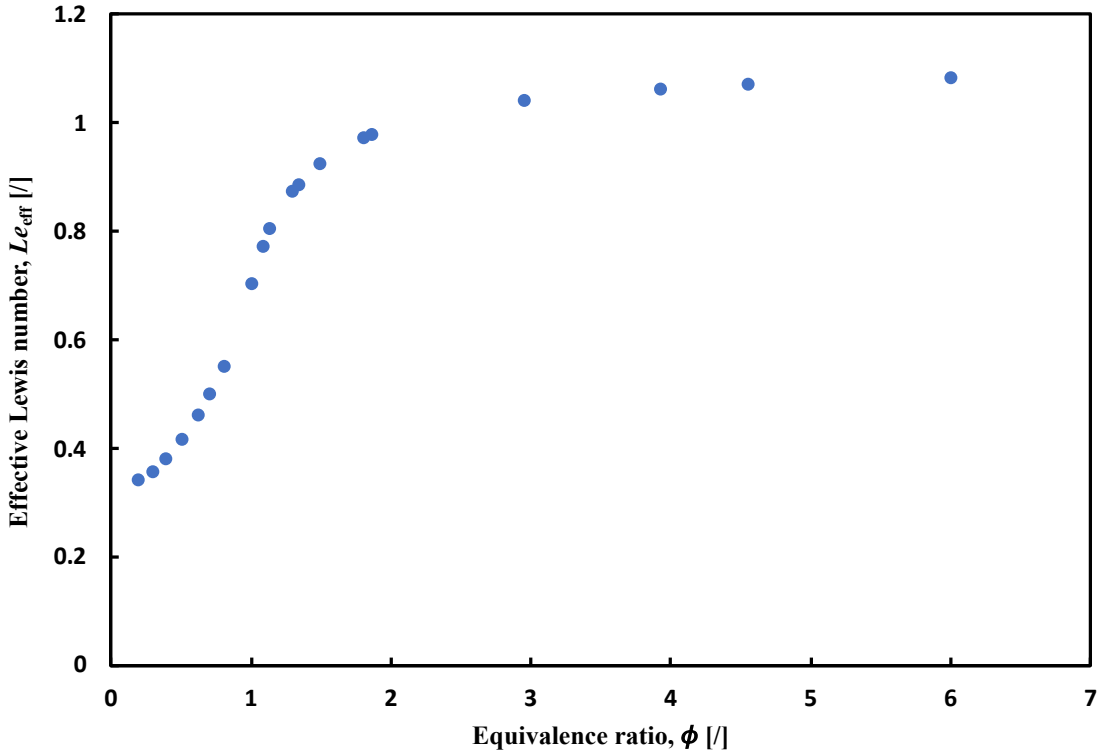

Fig. 11 Critical Péclet number versus equivalence ratio.

The critical Péclet number, Pe_{c}, which means the dimensionless critical flame radius, is defined as

$$Pe_{\mathrm{c}} = \frac{r_{\mathrm{c}}}{\delta} \tag{7}$$

Herein, the laminar flame thickness, δ, can be expressed as

$$\delta = \frac{T_{\mathrm{a}} - T_{\mathrm{u}}}{\left(\frac{\mathrm{d}T}{\mathrm{d}x}\right)_{\mathrm{max}}} \tag{8}$$

where T_{u} is the unburned gas temperature, and $(\mathrm{d}T/\mathrm{d}x)_{\mathrm{max}}$ is the maximum temperature gradient.

The Markstein number for the flame speed, Ma_{b}, which means the dimensionless Markstein length for the flame speed, is defined as

$$Ma_{\mathrm{b}} = \frac{L_{\mathrm{b}}}{\delta} \tag{9}$$

Figure 12 shows the critical Péclet number as a function of the Markstein number. Excluding the minimum point of $\phi = 0.2$, a linear relationship holds between the critical Péclet number and the Markstein number, which is $Pe_{\mathrm{c}} = 34.1Ma + 37.0$.

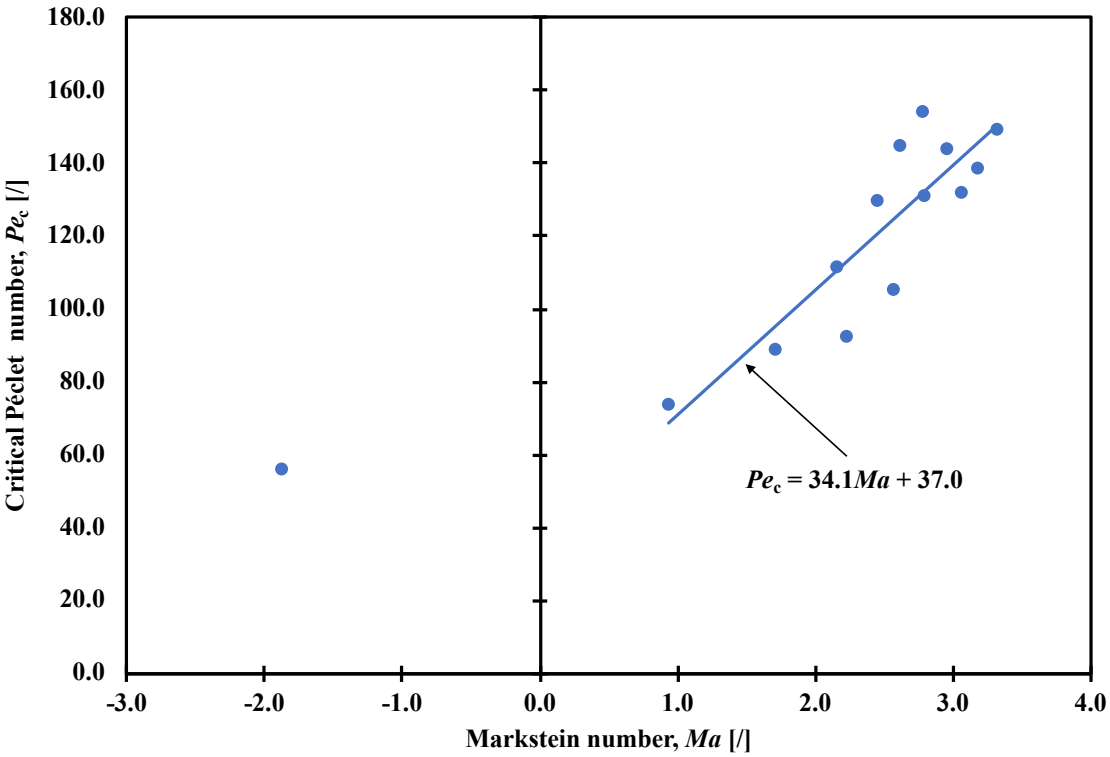

Fig. 12 Critical Péclet number vs Markstein number.

4 CONCLUSIONS

The experiments on unconfined explosions of hydrogen-oxygen mixtures were conducted by the soap bubble method. In this study, the laminar burning velocity, critical flame radii, critical Péclet number and Markstein number for hydrogen-oxygen mixtures were obtained at various equivalence ratios.

(1) The experimental values of the velocity were close to the calculation values of Chemkin-Pro with GRI Mech 3.0 reaction model. The values of laminar burning velocity in hydrogen-oxygen mixtures reaches a maximum at the near-stoichiometric mixture, although the maximum value of hydrogen-air mixtures peak on the rich side. The maximum velocity in hydrogen-oxygen mixtures is about 3 times faster than that of hydrogen-air mixtures.

(2) As the equivalence ratio decreases, the critical flame radius also decreases. Also, the critical flame radius in hydrogen-oxygen mixtures is smaller than in hydrogen-air mixtures.

(3) In the hydrogen-deficient gas, the effective Lewis number is less than 1.0 and thereby strong effect of diffusional-thermal instability forces on flame propagation. As a result, the flame front was wrinkled and the flame speed was accelerated at the early stage of flame propagation.

(4) As the equivalence ratio decreases, the Markstein length also decreases. This decreasing tendency of Markstein length with the equivalence ratio was similar to that of hydrogen-air mixtures.

(5) A linear relationship holds between the critical Péclet number and the Markstein number.

REFERENCES

1. Law, C.K., *Combustion physics*, 2006, Cambridge university press.
2. Williams, F. A., *Combustion theory*, 1985, Westview Press, U.K.
3. Kim, W., Mogi, T., Dobashi, R., Flame acceleration in unconfined hydrogen/air deflagrations using infrared photography, *Journal of Loss Prevention in the Process Industries* 26, 2013, 1501-1505.
4. Kim, W., Mogi, T., Dobashi, R., Fundamental study on accidental explosion behavior of hydrogen-air mixtures in an open space, *International Journal of Hydrogen Energy* 38, 2013, 8024-8029.
5. Clavin, P., Dynamic behaviour of premixed flame fronts in laminar and turbulent flows, *Prog. Energy Combust. Sci.* 11, 1985, 1-59.
6. Matalon, M., Matkowsky, B.J., Flames as gasdynamic discontinuities, *J. Fluid Mech*. 124, 1982, 239-259.
7. Kim, W., Mogi, T., Kuwana, K., Dobashi, R., Self-similar propagation of expanding spherical flames in large scale gas explosions, *Proceedings of the Combustion Institute* 35, 2015, 2051- 2058.
8. Kim, W., Mogi, T., Kuwana, K., Dobashi, R., Prediction model for self-similar propagation and blast wave generation of premixed flames, *International Journal of Hydrogen Energy* 34, 2015, 11087-11092.
9. Kim, W., Inamura, T., Mogi, T., Dobashi, R., Experimental investigation on the onset of cellular instabilities and acceleration of expanding spherical flames, *International Journal of Hydrogen Energy* 42, 2017, 14821-14828.
10. Kim, W., Sato, Y., Johzaki, T., Endo, T., Shimokuri, D., Miyoshi, A., Experimental study on self-acceleration in expanding spherical hydrogen-air flames, *International Journal of Hydrogen Energy* 43, 2018, 12556-12564.
11. Yaguchi, J., Kim, W., Mogi, T., Dobashi, R., Flame acceleration and blast wave of H_2-O_2-N_2-Ar mixtures in unconfined areas, *International Journal of Hydrogen Energy* 46, 2021, 12329-12337.
12. Muller, U. C., Bollig, M., Peters, N., Approximations for Burning Velocities and Markstein Numbers for Lean Hydrocarbon and Methanol Flames, *Combustion and Flame* 108, 1997, 349-356.
13. Bechtold, J. K., Matalon, M., The Dependence of the Markstein Length on Stoichiometry, *Combustion and Flame* 127, 2001, 1906-1913.